Scientific Knowledge Group

ISSN: 3068-2789

Research Article

Journal of All Physics Research and Applications

A Compound CNN-LSTM based Bearing Fault Diagnosis of Switched Reluctance Motor

Behara Santosh Sagar[1*], Prasad V Kane[2], Atul B Andhare[3], Makarand M Lokhande[4]

[1]*Research ScholarDept. of Mechanical Engineering VNIT, Nagpur, Maharashtra, India*
[2]*Assistant Professor Dept. of Mechanical Engineering VNIT, Nagpur, Maharashtra, India*
[3]*Professor Dept. of Mechanical Engineering VNIT, Nagpur, Maharashtra, India*
[4]*Associate Professor Dept. of Electrical Engineering VNIT, Nagpur, Maharashtra, India*

[*]Corresponding author:
Behara Santosh Sagar, Research ScholarDept. of Mechanical Engineering VNIT, Nagpur, Maharashtra, India.

ABSTRACT

Amid increasing efforts to reduce greenhouse gas (GHG) emissions, electric transportation solutions are being increasingly adopted by both individuals and businesses. Due to their simple construction and absence of permanent magnets, switched reluctance motors (SRMs) present a cost-effective alternative, positioning them as prime candidates for electric vehicle and traction applications. Despite the promising electrical fault tolerance of SRMs, their bearings are susceptible to brinelling and corrosion due to mechanical friction. This vulnerability underscores the need for reliable and automated bearing fault diagnosis technique. Moreover, the characteristic large torque ripple of SRMs complicates the application of conventional diagnosis methods, highlighting the necessity for specialized approaches. This paper presents a technical overview of traditional bearing fault diagnosis techniques and their inadequacy in dealing with complex and non-stationary conditions of SRMs. To overcome the problem, a novel compound neural network based intelligent fault diagnosis strategy is proposed which capitalizes on respective benefits of Convolutional Neural Networks and Long Short Memory Cells. The effectiveness of the proposed model is assessed via experiments carried out on a test rig containing defective bearings. It was observed that the proposed model was able to predict and classify the bearing defects with an exceptional accuracy of 95.16%. Additionally, t-distributed stochastic neighbor embedding (t-SNE) was employed to visualize and compare the learned feature distributions associated with various fault types.

Keywords: Switched Reluctance Motor, Torque Ripples, Bearing Fault Diagnosis, Convolutional Neural Networks.

Received: February 20, 2026;
Accepted: February 27, 2026;
Published: March 06, 2026

Introduction

In the recent past, there has been a considerable change in the technology trajectory of transportation sector. The need for greenhouse gas emission mitigation and a rapid growth in battery technology made the transportation industry more inclined towards the Electric Vehicles (EVs) [1]. Switched reluctance motors (SRMs) have been gaining increasing attention due to their simple construction and high fault tolerance. Unlike conventional motors, SRMs operate without permanent magnets, making them a cost-effective option for EV applications [2]. While SRMs are known for their high tolerance to electrical faults, their mechanical reliability remains a concern due to their inherently harsh operating conditions. The unique doubly salient structure and pulsed excitation of SRMs result in significant torque ripple, which contributes to elevated levels of vibration and acoustic noise [3]. These factors not only accelerate mechanical wear but also increase the likelihood of bearing-related faults, making effective fault diagnosis techniques essential for ensuring long-term performance and reliability in practical applications.

Citation: Behara Santosh Sagar (2026) A Compound CNN-LSTM Based Bearing Fault Diagnosis Of Switched Reluctance Motor. J All Phy Res Appli 2: 1-7.

With advancements in motor condition monitoring, various automated techniques have been proposed for bearing fault diagnosis. Recent studies have explored advanced approaches such as transient sound analysis, global spectrum methods, and multi-sensor data fusion using vibration and acoustic signals analysis [4-6]. However, due to the inherently high noise and electromagnetic interference associated with the operation of SRM, conventional bearing fault detection techniques such as Short-Time Fourier Transform (STFT) and Continuous Wavelet Transform (CWT) often prove inadequate. Additionally, techniques based on Motor Current Signature Analysis (MCSA) like Bi-spectrum analysis, Root-MUSIC, and angular resampling, primarily target induction and BLDC motors, not SRMs [7-9].

To address these challenges, traditional methods have been combined with machine learning (ML) classifiers. This, in other words is the intelligent fault diagnosis methodology. The traditional ML algorithms like Support Vector Machine (SVM), Stochastic Gradient Descent (SGD) Classifier, Principal Component Analysis (PCA) etc., have been in use for bearing fault diagnosis for decades [10-12]. Feature selection is a critical component in fault diagnosis methods based on ML framework. Feature selection is a process of selecting more relevant features for use in predictive model. This aids to make sense of the sought-after features and significantly influences the diagnostic accuracy. A three-phase sensitive Neighbor Component Analysis (NCA) is conducted to extract the significant feature parameters in [13]. Though ML based fault diagnostic techniques are promising tools, their further challenges are limited ability for learning non-linear relations of signals and need of human expertise for feature extraction.

Consequently, Deep learning (DL) models are increasingly favored for their superior performance in complex and noisy environments. Deep learning is a subset of artificial intelligent with a better abstract representation of data and a matured learning process. The effectiveness of enabling deep learning techniques for bearing fault diagnosis is summarized in [14]. CNNs and RNNs are the two main classes at the core of the deep learning revolution of intelligent fault diagnosis. CNNs process structured arrays of data as images through filters to extract the relevant features using convolution operations. CNN based bearing health prognostics perform well even in conditions that have no explicit characteristic frequencies. On the other hand, RNNs with recurrent connections on the hidden state have a high potential to capture the sequential information from input data. Long Short-Term Memory (LSTM), an important component of RNN, has become a hotspot in bearing fault diagnosis. These characteristics of CNNs and RNNs can be used for the bearing fault detection from the pre-processed sensory data.

Anurag et al. presented a Multi-sensor based Bayesian optimized Neural Network (Bonn) for bearing fault diagnosis of SRM in [15]. However, the feature extraction through the Bonn is preceded by the decomposition of acoustic and vibration data by the Hilbert Transform. A similar fault diagnosis method based on Vibrational Mode Decomposition (VMD) and improved CNN is proposed in [16]. An effective CNN steered with Wavelet Synchro squeezing Transform (WSST) is proposed for the bearing fault diagnosis of mid-drive SRM of an electric vehicle in [17]. A CWT based one-dimensional CNN with different kernel sizes is proposed in [18]. All these works relied on CNN. On the other hand, Lu et al. proposed a novel hierarchical algorithm based on stacked LSTMs in [19].

Avoiding the preprocessing procedures, many complex configured CNN classifiers based on attention mechanism and multi-channel signals were proposed in the literature [20-22]. While these deep architectures performed fairly well, they tend to be computationally heavy. In contrast to the state-of-the-art models which are all stand-alone models, the proposed model puts forward a novel compound CNN-LSTM network for bearing fault diagnosis of SRMs. The key contributions of this work are: (1) eliminating complex preprocessing, (2) using an adaptive architecture with fewer trainable parameters to reduce complexity and overfitting, and (3) achieving higher accuracy and reliability in SRM bearing fault diagnosis.

Theoretical Background

CNNs are a kind of feed-forward neural networks specially used for image related tasks such as pattern recognition and object classification. They are stacked layers of representations of input data in a hierarchical way. Though there are numerous variants of CNN architectures, they primarily consist of three types of layers: convolutional layer, pooling layer and fully connected layer. The typical architecture of a CNN is shown in Figure. 1.

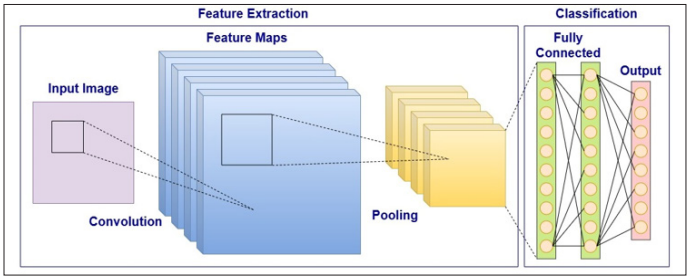

Figure 1: Typical stand-alone CNN architecture

Convolutional Layer

A convolutional layer, the core of a CNN, uses trainable kernels to extract local features and generate feature maps. These maps stack to form the layer's output, where each element acts like a neuron's output, connecting to pooling or fully connected layers. The convolution transformation formula is given by:

$$Z = f * (\Sigma W^T . X + b) \qquad (1)$$

where Z indicates the output component of the feature map, X is the input from the previous layer, W is the weight matrix, b is the bias and f is the non-linear activation function.

Pooling Layer

Pooling layers reduce the dimensionality of feature maps to lower computational load by summarizing features within receptive fields. The proposed architecture employs the max pool layer which is perhaps the most common and suggested method. The function of max pooling is represented as:

$$f^{(m)} = [f_1^{(m)} \ldots f_k^{(m)} \ldots f_K^{(m)}]^T \qquad (2)$$

where $f_k^{(m)} = \max_{x \in X_k} x$ is the maximum activation of the considered receptive field.

Fully Connected Layer and SoftMax Output layer

Extracted features from convolutional layers are passed to a fully connected layer. The fully connected layer is ideally a classifier layer which outputs a prediction. The activation function to be used in fully connected layer will depend upon the type of problem being solved, that is regression or classification. As this paper deals with multiclass fault classification task, a softMax activation is used to output normalized probabilities over the target classes. The softmax function is calculated as follows:

$$\sigma_j = \frac{\exp(z_j)}{\sum_{p=1}^{m} \exp(z_p)} \quad (3)$$

where σ_j is the output of softmax layer and z_j is the output of j^{th} neuron of classification layer.

Long Short-Term Memory (LSTM) Cell

Recurrent Neural Networks (RNNs) process sequential data by using hidden states to retain historical context. Long Short-Term Memory (LSTM) is an advanced variant of RNN that effectively captures long-term dependencies through gate mechanisms that regulate information flow. As shown in Figure. 2, LSTM uses trainable hidden and cell states (h_t and c_t) to learn temporal patterns via gated operations involving sigmoid activations and element-wise multiplication.

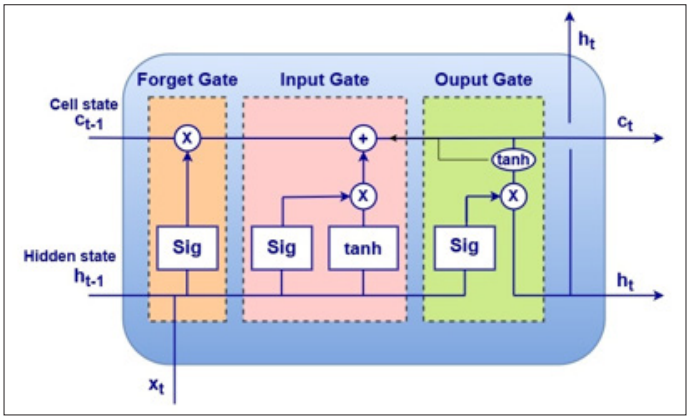

Figure 2: LSTM cell architecture

Proposed Methodology

The proposed methodology was designed to exploit the chief characteristics of the CNN and LSTM layers. It integrates the special feature extraction capability of CNN with temporal dynamics of LSTM to diagnose the bearing faults of SRM. The flowchart of the proposed model is shown in Figure. 3.

Data Preprocessing and Image Generation

Initially, the raw vibration signals are acquired at a 10 kHz sampling frequency from a motor operating at 20 Hz. Then, they are segmented using a fixed rectangular window of size, ensuring at least one complete bearing revolution (500 samples per revolution). These segments are then normalized between 0 and 1 and reshaped into 28 × 28 grayscale images, where each pixel value corresponds to the normalized amplitude. The

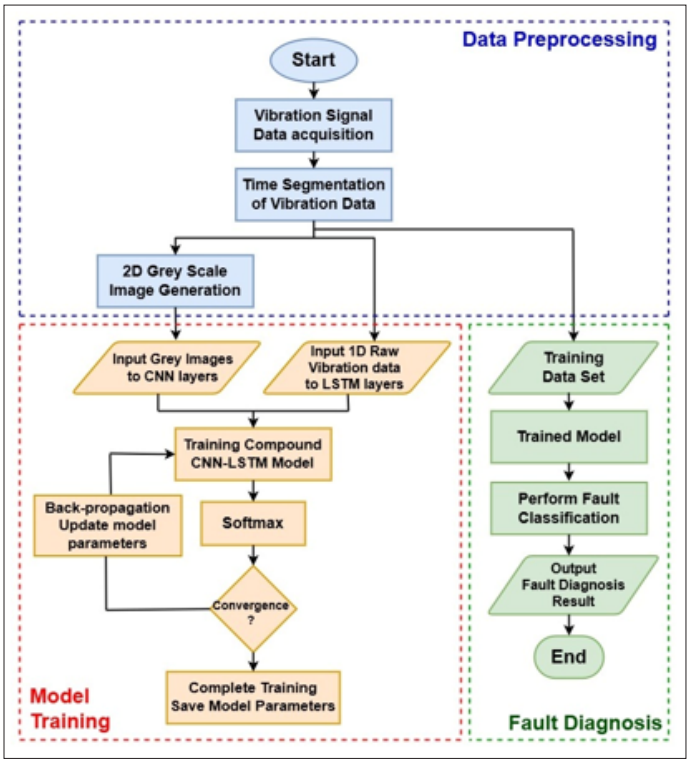

Figure 3: Flowchart of the proposed methodology

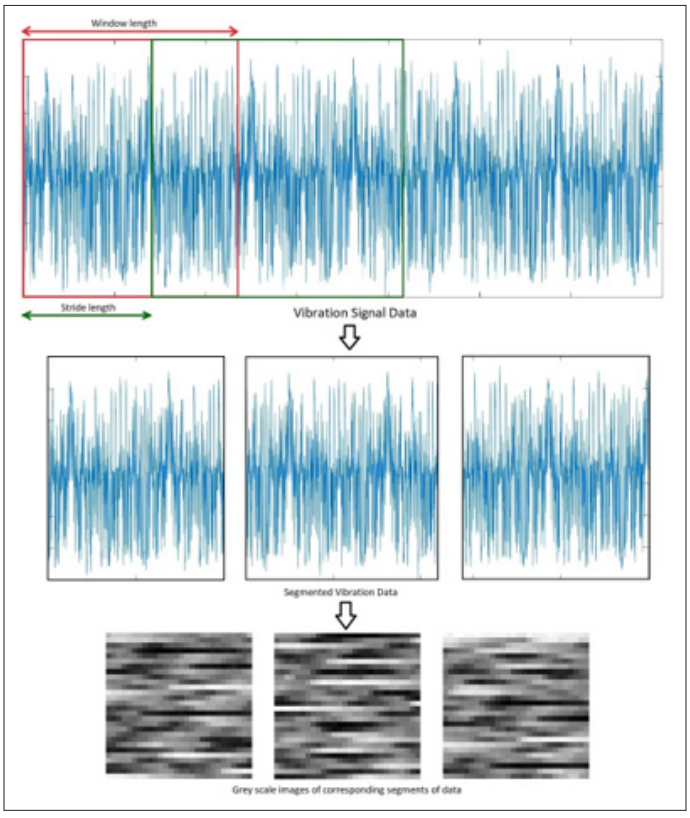

Figure 4: Processing of raw signal into grey scale images.

Proposed Compound CNN-LSTM Architecture

The architecture of the proposed network is inspired by the RNN-WDCNN (Wide and Deep CNN) architecture proposed in [23]. The details of the proposed compound CNN-LSTM architecture are shown in Figurre. 5. It basically has two branches; the first branch consists of three convolutional layers while the second branch contains three LSTM layers.

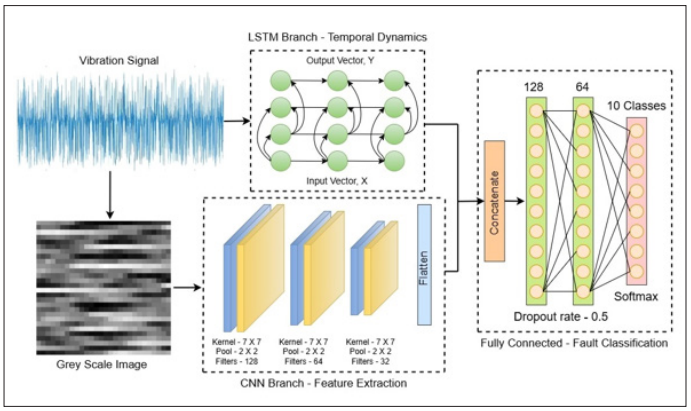

Figure 5: Architecture of the proposed compound CNN-LSTM model.

The CNN branch processes grayscale vibration images through three convolutional layers with a fixed kernel size of 7 X 7. The first, second and third layers use 128, 64, and 32 filters respectively, that reflects the hierarchical feature extraction from finer to broader image regions. Each convolutional layer is followed by a 4 X 4 max-pooling layer for dimensionality reduction. While effective at extracting discriminative features, the CNN alone struggles to capture long-range dependencies in noisy vibration signals. To address this, an LSTM branch is incorporated, which models temporal dynamics and long-term dependencies by processing the raw time-series signal in parallel. This combined CNN-LSTM architecture enhances feature learning and improves overall performance.

Finally, the compound architecture is followed by two fully connected layers with 128 and 64 neurons and an output SoftMax layer for fault classification. ReLU activation is employed throughout the model due to its computational efficiency and mitigation of the vanishing gradient problem. Model parameters and hyperparameters, including batch size and learning rate, are chosen to balance the tradeoff between training speed and classification accuracy.

Application To Srm Bearing Fault

Experimental Setup and Fault Seeding

The experiments were conducted using a 1-hp 4 phase 8/6 SRM coupled with a spring-based loading system and a programmable STM32F4-WJ digital signal processor controller. The complete arrangement of experimental test rig is shown in Figure. 6.

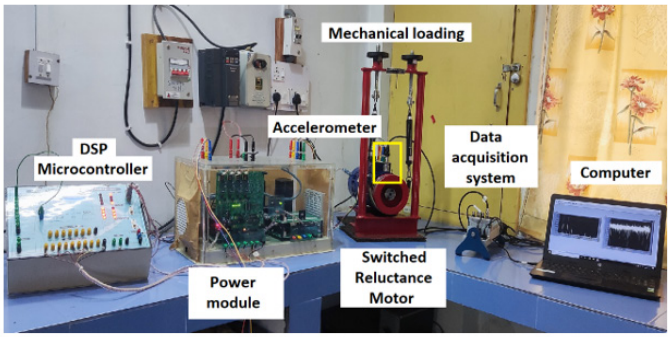

Figure 6: Experimental test rig.

Vibration signals were acquired using a PCB Piezotronics 356A45 accelerometer (100 mV/g sensitivity) at a 10 kHz sampling rate. Data were logged to a PC via a National Instruments NIDAQ9178 system and NI LabVIEW software. Motor speed was measured using a built-in tachometer with an LCD display. SKF deep groove ball bearings (6204-2Z/C3) with a 20 mm bore, 47 mm outer diameter, and 14 mm width were used. Three fault types (inner race, outer race, roller ball) were seeded via EDM at severity levels of 0.5, 0.7, and 0.9 mm as shown in Figure. 7. Vibration data were recorded under healthy and faulty conditions across five load levels (0%, 25%, 50%, 75%, 100% rated load), resulting in 50 distinct tests.

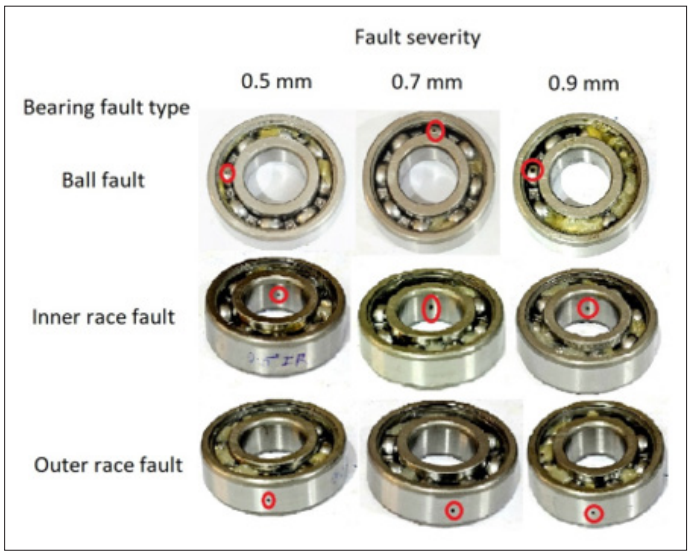

Figure 7: Different types and severities of faults.

Dataset Details and Label Notations

The acquired raw vibration data is processed as explained in the subsection 3.1 to generate the grey scale images. As mentioned earlier, the experimental data was collected from the accelerometer at a sampling frequency of 10 kHz and signal time of 2 seconds. Thus, for each condition there will be a total of 20000 data points. Finally, the combined time signals (combined signals of 10 classes) resulted in the generation of 6620 gray scale images. Of which 70% of the images were used for training and the remaining 30% for testing. The details of the transformed grey scale image count and notations for different kinds of faults and severity levels are given in **Error! Reference source not found..**

Fault Diagnosis Results

The certainty of the fault identification and classification ability of the proposed model is verified with a series of experiments. The standard categorical cross-entropy function given in Eq. (4) is used to optimize the learning parameters. Accuracy is used as the performance metric to quantify all the aspects of the classifier performance, which is widely used in literature.

$$H(X) = -\sum_{K} p(x_i).\log q(x_i) \quad (4)$$

where $p(x_i)$ and $q(x_i)$ denote the target and estimated probabilities of the i^{th} class and K is the total number of classes.

Table 1: Details of the adopted notations and the grey scale image count

Fault type / Condition	Fault severity	Class label	Fault notation	Number of Images	
				Training	Testing
Healthy	-	1	H	463	199
Rolling element (Ball) Defect	0.5 mm	2	0.5B	463	199
	0.7 mm	3	0.7B	463	199
	0.9 mm	4	0.9B	463	199
Inner race defect	0.5 mm	5	0.5I	463	199
	0.7 mm	6	0.7I	463	199
	0.9 mm	7	0.9I	463	199
Outer race defect	0.5 mm	8	0.5O	463	199
	0.7 mm	9	0.7O	463	199
	0.9 mm	10	0.9O	463	199
			Total	**6620**	

Learning Graphs

The compound CNN-LSTM model was trained using TensorFlow v2.13.0 with the Keras API, employing a batch size of 200, a learning rate of 0.001, and the Adam optimizer. Hyperparameters were selected by tuning default values while monitoring convergence behavior. Training and validation accuracy and loss curves are shown in Figure. 8, with epochs on the horizontal axis and performance metrics on the vertical. The model gradually learned data complexities, reaching a peak accuracy of 95.16%. Validation loss was unstable until approximately the 2000th iteration but stabilized thereafter. Training was terminated at 2800 epochs, when the loss dropped below 0.2 and accuracy plateaued, and the final model was saved.

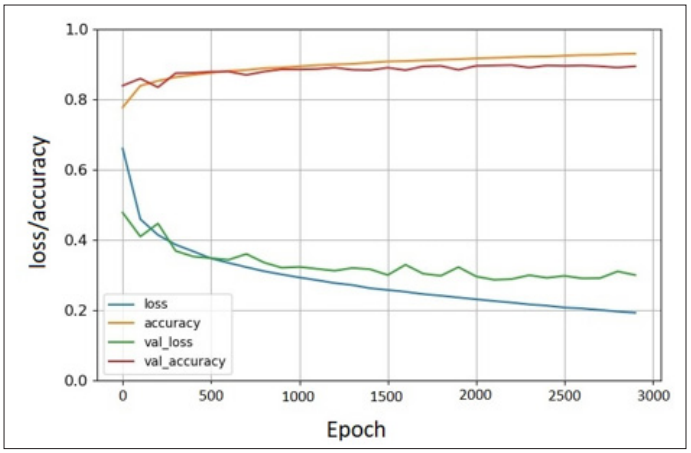

Figure 8: Learning curves of the proposed model

One more notable observation is the gap between training and validation loss, indicating the absence of overfitting. This suggests that the model generalizes well to unseen instances, making it suitable for fault detection.

Confusion Matrix Analysis

The comprehensive performance of the designed compound CNN-LSTM classifier model is evaluated using the multi-class confusion matrix. The confusion matrix is a succinct way of evaluating a classifier model by mapping the expected outcomes to the predicted outcomes. The diagonal elements of the confusion matrix represent the number of correctly classified instances. The obtained accuracies after processing the test data through the model are well represented by the normalized confusion matrix in Figure. 9. It is evident from the confusion matrix that the diagnosis accuracies of each of the distinctive conditions of the bearings are promising. It shows that seven of the ten conditions (including the healthy class) have accuracies more than 98% which is exceptional.

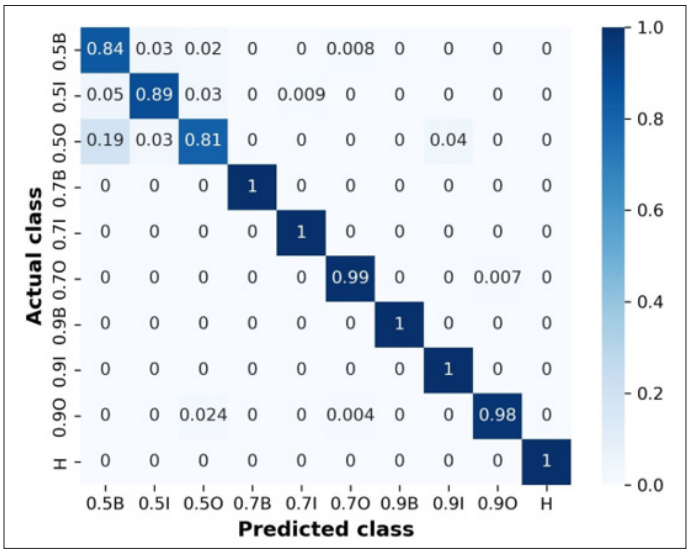

Figure 9: Normalized confusion matrix

As mentioned in the previous sub-section, the overall classification accuracy of the model is about 95.16%. On the contrary, it can be noted that the performance of the model is mediocre for the fault of size 0.5 mm, with slightly lesser accuracies of 84.17%, 89.21% and 81.66% for the ball fault, inner race and outer race faults respectively. Finally, we remark that the generalization of the proposed compound network was bound to the mentioned accuracies and remained unimproved regardless the change of learning rates and batch sizes.

Feature Visualization of Fault Scenarios

As accuracy alone does not fully reflect a model's ability to learn distinct class boundaries, t-distributed stochastic neighbor embedding (t-SNE) was employed for dimensionality reduction

and feature visualization. As shown in Figure. 10, the proposed network effectively clusters feature corresponding to different fault types, indicating strong discriminative capability. However, minor overlaps are observed among the 0.5 mm fault classes, highlighting the challenge of detecting early-stage defects in SRM bearings. Additionally, the clear separation and stretching between clusters suggest that the learned features possess further potential to enhance fault classification performance.

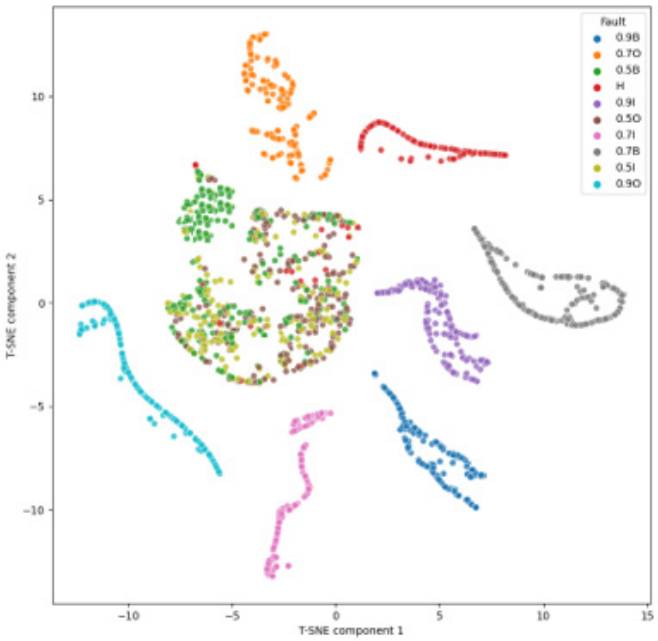

Figure 10: Data distribution after t-SNE dimensionality reduction

Conclusion

Switched Reluctance Motors, despite their structural simplicity, present significant challenges in diagnosing bearing faults. An attempt is made in this work to develop a compound network methodology that leverages CNN's spatial feature extraction and LSTM's temporal modeling capabilities. Experimental validation demonstrated that the proposed compound CNN-LSTM architecture achieved a high classification accuracy of 95.16%, outperforming traditional methods and standalone CNN or RNN models in both efficiency and effectiveness. However, performance degradation was observed in detecting incipient faults, particularly for defects of 0.5 mm severity, as evidenced by confusion matrix analysis. Future work will focus on developing neural network models that incorporate vibro-acoustic multisensory data fusion to overcome this limitation. Given the flexibility and purely data-driven nature of the proposed model, the underlying method can be extended to fault diagnosis in other mechanical and electrical components.

References

1. Yu Gan, Michael Wang, Zifeng Lu, Jarod Kelly (2021) Taking into account greenhouse gas emissions of electric vehicles for transportation de-carbonization. Energy policy 155: 112353.
2. Yuanfeng Lan, Yassine Benomar, Kritika Deepak, Ahmet Aksoz, Mohamed El Baghdadi, et al. (2021) Switched reluctance motors and drive systems for electric vehicle powertrains: State of the art analysis and future trends, Energies 14: 2079.
3. Gaoliang Fang, Filipe P Scalcon, Dianxun Xiao, Rodrigo P Vieira, Hilton A Gründling, et al. (2021) Advanced control of switched reluctance motors (SRMs): A review on current regulation, torque control and vibration suppression. IEEE Open Journal of the Industrial Electronics Society 2: 280-301.
4. Siliang Lu, Xiaoxian Wang, Qingbo He, Fang Liu, Yongbin Liu, et al. (2016) Fault diagnosis of motor bearing with speed fluctuation via angular resampling of transient sound signals. Journal of Sound and Vibration 385: 16-32.
5. Jinane Harmouche, Claude Delpha, Demba Diallo (2014) Improved fault diagnosis of ball bearings based on the global spectrum of vibration signals. IEEE Transactions on Energy Conversion 30: 376-383.
6. Xiaoxian Wang, Siliang Lu, Kang Chen, Qunjing Wang, Shiwu Zhang, et al. (2021) Bearing fault diagnosis of switched reluctance motor in electric vehicle powertrain via multisensor data fusion. IEEE Transactions on Industrial Informatics 18: 2452-2464.
7. Alwodai Ahmed, Wang Tie, Chen Zhi, Gu Fengshou, Cattley Robert, et al. (2013) A study of motor bearing fault diagnosis using modulation signal bispectrum analysis of motor current signals. Journal of Signal and Information Processing 4: 72.
8. Ahmed Hamida Boudinar, Noureddine Benouzza, Azeddine Bendiabdellah, Mohammed-El-Amine Khodja (2016) Induction motor bearing fault analysis using a root-MUSIC method. IEEE Transactions on Industry applications 52: 3851-3860.
9. Siliang Lu, Jie Guo, Qingbo He, Fang Liu, Yongbin Liu, et al. (2016) A novel contactless angular resampling method for motor bearing fault diagnosis under variable speed. IEEE Transactions on Instrumentation and Measurement 65: 2538-2550.
10. PK Kankar, Satish C Sharma, SP Harsha (2011) Fault diagnosis of ball bearings using machine learning methods. Expert Systems with applications 38: 1876-1886.
11. Xiao Zhang, Boyang Zhao Yun Lin (2021) Machine learning based bearing fault diagnosis using the case western reserve university data: A review. Ieee Access 9: 155598-155608.
12. EP de Moura, CR Souto, AA Silva, MAS Irmão (2011) Evaluation of principal component analysis and neural network performance for bearing fault diagnosis from vibration signal processed by RS and DF analyses. Mechanical Systems and Signal Processing 25: 1765-1772.
13. Bodi Cui, Yang Weng, Ning Zhang (2022) A feature extraction and machine learning framework for bearing fault diagnosis. Renewable Energy 191: 987-997.
14. Shen Zhang, Shibo Zhang, Bingnan Wang, Thomas G Habetler (2020) Deep learning algorithms for bearing fault diagnostics-A comprehensive review. IEEE access 8: 29857-29881.
15. Anurag Choudhary, Tauheed Mian, Shahab Fatima, Bijaya Ketan Panigrahi (2023) Multi Sensor based Bearing Fault Diagnosis of Switched Reluctance Motor for Electric Vehicle. Proceedings of the 2023 6th International Conference on Electronics, Communications and Control Engineering 257-263.

16. Zhenzhen Jin, Diao Chen, Deqiang He, Yingqian Sun, Xianhui Yin, et al. (2023) Bearing fault diagnosis based on VMD and improved CNN. Journal of Failure Analysis and Prevention 23: 165-175.
17. Anurag Choudhary, Tauheed Mian, Shahab Fatima, BK Panigrahi (2023) Fault diagnosis of electric two-wheeler under pragmatic operating conditions using wavelet synchrosqueezing transform and CNN. IEEE Sensors Journal 23: 6254-6263.
18. Jun Zhang, Yang Zhou, Bing Wang, Ziheng Wu (2021) Bearing fault diagnosis base on multi-scale 2D-CNN model, in 2021 3rd International Conference on Machine Learning. Big Data and Business Intelligence (MLBDBI) 72-75.
19. Lu Yu, Jianling Qu, Feng Gao, Yanping Tian (2019) A novel hierarchical algorithm for bearing fault diagnosis based on stacked LSTM. Shock and Vibration 2756284.
20. Huan Wang, Zhiliang Liu, Dandan Peng, Zhe Cheng (2022) Attention-guided joint learning CNN with noise robustness for bearing fault diagnosis and vibration signal denoising. ISA transactions 128: 470-484
21. Jianguo Yin, Gang Cen (2022) Intelligent motor bearing fault diagnosis using channel attention-based CNN. World electric vehicle journal 13: 208.
22. Serkan Kiranyaz, Onur Avci, Osama Abdeljaber, Turker Ince, Moncef Gabbouj, et al. (2021) 1D convolutional neural networks and applications: A survey. Mechanical systems and signal processing 151: 107398.
23. Alex Shenfield, Martin Howarth (2020) A novel deep learning model for the detection and identification of rolling element-bearing faults. Sensors 20: 5112.